Kriosfera Zemli, 2021, vol. XXV, No. 3, pp. 43–51

CALCULATION OF THE HEAT BALANCE COMPONENTS OF THE ALDEGONDA GLACIER (WESTERN SPITSBERGEN) DURING THE ABLATION PERIOD ACCORDING TO THE OBSERVATIONS OF 2019

U.V. Prokhorova[1], A.V. Terekhov[1], B.V. Ivanov[1,2], S.R. Verkulich[1]

[1] *Arctic and Antarctic Research Institute, Bering str. 38, Saint Petersburg, 199397, Russia; uliana@niersc.spb.ru*
[2] *Saint Petersburg State University, Universitetskaya emb. 7/9, Saint Petersburg, 199011, Russia*

Surface heat balance components have been calculated for the mountain valley Aldegonda Glacier (West Spitsbergen Island) based on a physical model with distributed parameters. The meteorological and actinometric observations on the glacier during the ablation period of 2019, a digital elevation model, as well as the remote sensing data needed for assessment of the reflective characteristics of the surface have been used as the input data. As a result of modeling, a spatial distribution of the values of the heat flux spent on melting with a resolution of one day has been obtained. According to the calculations, the average radiation balance for the period has been 89 W/m^2, which is approximately an order of magnitude higher than the heat inflow from turbulent flows (11 W/m^2). The obtained results have been verified using data on the glaciological mass balance monitoring based on ablation stakes. Predicted thickness of melted ice layer is in good agreement with the measurements on ablation stakes. The model systematically overestimates the magnitude of ice melt, but the glacier-average value remains within the confidence interval of the observed value.

Key words: *Svalbard, mountain glacier, glacier ablation, heat balance, physical modelling.*

INTRODUCTION

Over the last decades a steady warming is observed in the Svalbard Archipelago area. Rates of warming are higher than the world average due to the 'Arctic amplification' effect [*Nordli et al., 2014; Gjelten et al., 2016; Isaksen et al., 2016*]. The amount of atmospheric precipitation also tends to increase, but to a much lesser extent [*Førland et al., 2020*], as a result the winter snow accumulation on the archipelago glaciers is not able to compensate summer melting. Therefore, the total mass balance of the Svalbard Archipelago glaciers demonstrates a negative trend and, according to the latest estimate, is -7 ± 4 billion tons/year (excluding the icebergs calving from outlet glaciers) [*Schuler et al., 2020*]. In light of these facts, monitoring and forecasting the mass-balance characteristics of the archipelago glaciers are undoubtedly relevant scientific issues.

At present, the models based on empirical dependence of melting on air temperature are mainly used to assess the ablation of Arctic glaciers [*Krenke, Khodakov, 1966; Ohmura, 2001; Hock, 2003; Chernov et al., 2019*] and providing an integral estimate of ablation over the entire glacier, and the models based on the glacier heat balance equation [*Hock, 2005*]. The latter require a large number of spatially distributed parameters and are used less often due to the smaller number of actinometric observations carried out on glaciers, as well as because of the difficulties in assessing the turbulent flows and reflective characteristics of the surface. Nevertheless, heat-balance models for seasonal and interannual estimates of mass balance were applied, demonstrating good results for glaciers in northern Canada [*Wheler, Flowers, 2011*], in the Swiss Alps [*Klok, Oerlemans, 2002*], in the Caucasus [*Voloshina, 1966, 2001; Retz et al., 2011; Toropov et al., 2018*] and in the Western Spitsbergen [*Arnold et al., 2006; Svyaschennikov, Ragulina, 2010; Van Pelt, 2012; Karner et al., 2013*].

Heat-balance ablation models based on the thermodynamic approach allow to characterize quantitatively the contribution of a particular meteorological parameter to melting on the glacier surface and to reveal the mechanisms of interaction between elements of the climate system (cryosphere–atmosphere).

This paper presents the results of assessing the components of the heat balance of the Aldegonda Glacier surface, based on data from field experiments in August 2019. The heat balance has been calculated using daily time-step heat balance model. The spatial distribution of ablation obtained by simulation was compared with the data of glaciological measurements using ablation stakes for the same period. The Aldegonda Glacier is typical in size and altitude range of the West Spitsbergen central part, where glaciation is decreasing most rapidly, so obtained results can be extrapolated to the entire mountain-glacial system of the archipelago.

OBJECT OF STUDY

The mountain-valley Aldegonda Glacier (in Norwegian, *Aldegondabreen*) is located on the western coast of the Grønfjorden Bay, West Spitsbergen Island (Fig. 1). Almost the entire glacier surface is located in the altitude interval from about 120 to 450 m above sea level; its maximum elevation reaches 600 m. The glacier surface is rather homogeneous in terms of relief and is weakly dissected, mainly by se-

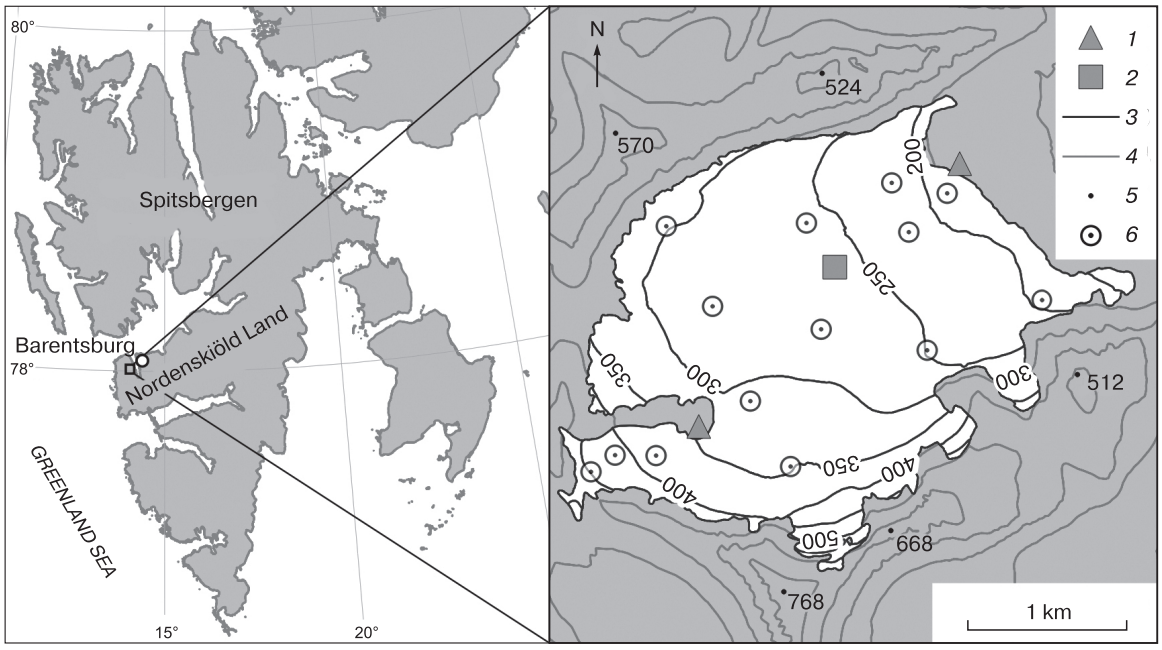

Fig. 1. Aldegonda Glacier and the observation network on it:

1 – permanent automatic weather stations; *2* – heat balance mast in August 2019; *3* – isohypses of the glacier surface; *4*, *5* – isohypses and altitudes of the surrounding topography (heights are given from sea level according to the ArcticDEM for 2013); *6* – ablation stakes.

veral longitudinal streams. There are no icefalls or sharp slope changes expect several crevasses in the very upper reaches. According to the authors' observations, there are no signs of intense ice movement. The small area of the glacier (5.54 ± 0.28 km^2 at the time of the study) and the proximity to Barentsburg settlement, where the logistics base of the Russian Scientific Center on the archipelago is located, predetermined its choice as an object of annual mass balance monitoring based on measurements using ablation stakes. The latter makes it possible to verify the simulation results presented in this work. The altitude range of the glacier is conventionally divided into fifty-meter intervals; fourteen ablation stakes are placed on the glacier surface so that at least one of them falls into each of the intervals (Fig. 1). In the largest by area altitudinal intervals, several stakes are installed in order to take into account possible uneven shading by rocky framing and uneven topography. That makes it possible to analyze not only the dependence of the melting layer thickness on altitude, but also the features of its spatial distribution.

According to the Roshydromet weather station located in Barentsburg, in recent decades the mean surface air temperature in the summer and early autumn (June–September) is positive. Around the same period, active melting of glaciers also occurs in the area of Grønfjorden Bay. On the Aldegonda glacier, the snow cover disappears almost completely by the third decade of July, the entire ice surface is below the snow line by the end of summer.

MATERIALS AND METHODS

The assessment of the heat balance components and the ablation values on the surface of the Aldegonda Glacier in August 2019 has been carried out on the basis of a physical model with spatially distributed parameters. The input meteorological data were obtained during field observations performed by the authors in the Russian Scientific Arctic Expedition on the Svalbard Archipelago (RAE-S), of the State Scientific Center of the Russian Federation 'Arctic and Antarctic Research Institute' (SSC RF 'AARI') in August 2019.

Field data and their interpolation. Heat balance observations were carried out in August in the absence of snow cover on the surface.

The bulk of the input data for modeling has been obtained using a heat balance mast (HBM) installed in the central part of the glacier, at an altitude of about 260 m above sea level for the period from 2 to 26 August 2019. The site had been considered as representative because the glacier surface is as homogeneous as possible, relatively flat and not shaded by slopes (Fig. 1). The HBM was equipped with actinometric sensors to assess the shortwave and longwave components of the surface radiation balance. Those

include: Yanishevsky pyranometers M-80, which record the total (incoming) and reflected solar radiation within the spectral range of 330–2800 nm, as well as APOGEE infrared radiometers, which measure the temperature (°C) of the glacier surface and air; on the basis of the latter, the downwelling longwave radiation of the atmosphere has been calculated. To assess the turbulent heat transfer between the glacier surface and the atmosphere, the HBM was equipped with the air temperature, atmospheric pressure, relative humidity and wind speed sensors from the HOBO automatic weather station kit. The data were recorded by LICOR-1400 and Campbell Scientific loggers each 5 minutes.

Extrapolation of data on air temperature, relative humidity and atmospheric pressure to the entire glacier surface was carried out using the ArcticDEM digital elevation model (DEM) for 2013, covering without gaps the entire glacier surface area and adjacent valley sides, as well as using the values of the vertical gradients of the indicated meteorological parameters. Vertical gradients were estimated using two HOBO automatic weather stations (Fig. 1) installed on moraine-covered rock outcrops in the lower part of the glacier and in its uppermost part. The weather stations were equipped with the temperature, relative humidity, wind speed and direction, atmospheric pressure sensors. The stations operate year-round, with hourly measurements.

One of the few meteorological parameters that is entered into the model as lumped, that is, non-distributed over the entire surface of the glacier, is the near-surface wind speed (modeling the wind field over the glacier surface is an independent and extremely difficult task). The temperature of the melting glacier surface, due to its insignificant changes (from –0.4 to +0.3 °C) according to measurements on the HBM (Fig. 2), was taken constant and equal to 0 °C. The partial pressure was also taken as a constant, equal to 6.11 hPa.

Model-based calculation of melting values. To estimate the values of melting, the equation of the surface heat balance is used. The heat losses on melting are estimated as the residual term of the equation:

$$A = Q(1 - \alpha) + I + P + LE + G, \qquad (1)$$

where: A is heat losses for melting; Q is incoming shortwave radiation; α is albedo of the underlying surface; I is longwave radiation balance; P and LE are vertical turbulent fluxes of sensible and latent heat; G is heat flux directed into the glacier. The simulation time step is equal to one day, so all the flows in the equation (1) are calculated as daily-average ones. The calculation of each of the components is described below.

The shortwave balance, represented in the equation (1) by the $Q(1 - \alpha)$ term, is determined by the flow of incoming shortwave radiation (Q) and the reflective characteristics of the surface (α). To spread the values of the incoming flow (Q) obtained at the HBM installation point to the entire glacier surface, it is necessary to take into account the effects of shading and morphometry (slope and exposure). The authors used the 'Potential Incoming Solar Radiation' algorithm, implemented in the GIS SAGA, which makes it possible to estimate the illuminance of the surface depending on astronomical factors (zenith and hour angle of the Sun, the time of sunrise and sunset) and topography itself (slope, exposure and shading by the surrounding terrain) [*Böhner, Antonić, 2009*]. A 15-minutes time-step was used. The Q value measured on the glacier surface was compared with that obtained at the corresponding point of the model, the scale factor was calculated, and on its basis the model field was corrected. The obtained spatial distribution of the average daily flux of shortwave radiation was used in further calculations.

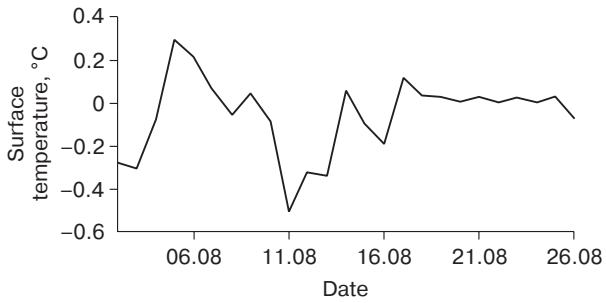

Fig. 2. Day-to-day variability of the surface temperature of the Aldegonda Glacier during 2019 observation period at the point of HBM installation.

The glacier surface albedo (α) is extremely heterogeneous in space and it can vary significantly over time depending on the presence or absence of fresh snow, as well as on the natural pollution of the glacier surface [*Ivanov, Svyashchennikov, 2015*]. Therefore, the point or route measurements on the glacier surface do not allow us to correctly assess these features. A logical solution is to estimate the spatial distribution of the albedo values using satellite data. For that purpose, cloudless images from Landsat-8 Level 2 collection with a spatial resolution of 30 m have been used. The set of images for each date contains data from seven spectral channels of the optical range, converted into the values of surface reflectance (surface spectral brightness coefficients, in Russian) by eliminating atmospheric effects and the difference in illuminance.

To obtain an integral value through the values of the surface spectral albedo in individual wave ranges, the formula proposed in [*Liang, 2001*] and adapted for the Landsat-8 satellite [*Naegeli et al., 2017*] had been used. The formula is a multiple linear regression

equation in which five of the seven Landsat-8 spectral bands are predictors:

$$\alpha = 0.356b_2 + 0.130b_4 + 0.373b_5 + \\ +0.085b_6 + 0.072b_7 - 0.0018, \quad (2)$$

where b_i is the value of surface reflectance in the i-th spectral channel of Landsat-8. It has been revealed in [*Naegeli et al., 2019*] that such a calculation allows to obtain reliable value of mountain-glacier surface albedo. The integral albedo values for the periods between imagery acquisition were obtained by linear interpolation of the images closest in time.

The longwave budget (I) or effective radiation of the earth's surface – the difference between the upward and downward longwave radiation – was calculated using the method described in [*König-Langlo, Augsteine, 1994*]. In accordance with that approach, the longwave budget of the underlying surface is:

$$I = \varepsilon\sigma T_s^4 - \varepsilon_a(n,T,e)\sigma T^4, \quad (3)$$

where T_s is surface temperature (K); ε – radiant emissivity of the surface, taken for ice equal to 0.98; σ is the Stefan-Boltzmann constant equal to $5.669 \cdot 10^{-8}$ W/(m^2·K^4).

However, since during the melting period the glacier surface temperature in the used model is 0 °C according to the observation data (Fig. 2), the upwelling radiation (the first term in the equation (3)) has assumed to be constant and equal to 316 W/m^2.

The second term in the equation (3) is the atmospheric downwelling radiation, where ε_a is the radiant emissivity of the atmosphere, which is a function of the cloud cover (n), air temperature (T), and water-vapor pressure (e) at a 2 m height. A comprehensive review of existing approaches to assessing the atmosphere radiant emissivity is given in [*König-Langlo, Augsteine, 1994*]. We used an empirical relationship adapted by the authors to the conditions of Svalbard Archipelago:

$$\varepsilon_a = a_k + b_k n,$$

where n is the total cloud cover (in unit fractions) according to visual observations; a_k and b_k are empirical coefficients ($a_k = 0.765$, $b_k = 0.22$). To interpolate the values over the entire glacier surface, the vertical air temperature gradient was also taken into account, which was calculated using the AMS data recorded in the upper and lower parts of the glacier (Fig. 1). The upper AMS is installed at a small moraine, and the lower AMS is located in close proximity to the glacier, so there is every reason to assume that the measured temperature gradient is the same as that above the ice.

To calculate the turbulent fluxes of sensible (P) and latent (LE) heat, the method described in [*Munro, 1990*], based on the Monin–Obukhov semi-empirical theory of turbulence, was used. That approach has been successfully applied to simulate the melting of mountain glaciers, and the results are presented in a number of publications [*Hock, 2005; Wheler, Flowers, 2011*]. To estimate the P and LE values, aerodynamic formulas are used, which include the wind speed, temperature and relative humidity of air values at the same height above the surface (z) and the values of meteorological characteristics on the surface (s):

$$P = C_H c_p \rho_a u_z (T_z - T_s),$$

$$LE = C_E L_v \rho_a u_z \left(\frac{0.622}{p}\right)(e_z - e_s),$$

where C_H and C_E are the coefficients of turbulent heat transfer; ρ_a is the air density calculated on the basis of its temperature and pressure; $c_p = 1010$ J/(kg·K) is the air specific heat capacity; $L_v = 2.514 \cdot 10^6$ J/kg is the latent heat of vaporization. The wind speed (u_z), the air temperature (T_z) and the pressure (p) have been measured at a height of $z = 1.6$ m. T_s and e_s are correspondingly the temperatures of the melting surface and the water-vapor pressure near it. The partial pressure of water vapor at height of z is calculated on the base of measured relative humidity.

Turbulent heat transfer coefficients are calculated by the following formulas [*Hock, Holmgren, 1996*]:

$$C_{H,E} = \\ = \frac{k^2}{\left[\ln(z/z_M) - \Psi_M(z/L)\right]\left[\ln(z/z_{H,E}) - \Psi_{H,E}(z/L)\right]}, \quad (4)$$

where $k = 0.4$ is Karman constant; z_M and $z_{H,E}$ are the surface roughness for wind, heat and water vapor; Ψ_M, and $\Psi_{H,E}$ are universal functions; L is the Monin–Obukhov parameter. The roughness values are given by the authors as $z_M = 10$ mm, $z_{H,E} = z_M/100$. These values have been chosen by the authors based on a review of similar calculations performed for the surface conditions of other glaciers [*Wheler, Flowers, 2011*].

The Ψ_M and $\Psi_{H,E}$ function values have been calculated in accordance with the work [*Beljaars, Holtslag, 1991*] and characterize the conditions of stable stratification of near-surface air layer prevailing over the glacier surface in the summer season:

$$-\Psi_M = \frac{az}{L} + b\left(\frac{z}{L} - \frac{c}{d}\right)\exp\left(-d\frac{z}{L}\right) + \frac{bc}{d},$$

$$-\Psi_{H,E} = \left(1 + \frac{2az}{3L}\right)^{1.5} + b\left(\frac{z}{L} - \frac{c}{d}\right)\exp\left(-d\frac{z}{L}\right) + \frac{bc}{d} - 1,$$

where a, b, c, d are empirical coefficients equal to 0.7, 0.75, 5.0, 0.35, respectively. Wheler and Flowers [*2011*] have demonstrated that these values of the universality functions give an acceptable result in ablation simulations.

Calculations using the formulas above require the value of the Monin–Obukhov parameter (L),

which has been determined using the following expressions:

$$L = \frac{\rho c_p u_*^3 T_z}{kgP}; \quad (5)$$

$$u_* = \frac{ku_z}{\ln(z/z_M) - \Psi_M}, \quad (6)$$

where u_* is dynamic velocity.

Thus, the calculation of the Monin–Obukhov parameter requires a fixed value of the unknown sensible heat flux. In such cases, an iterative procedure is used. At the first step, the ratio z/L (stability function) is assumed to be zero, which simplifies the formula (4). Based on that, an approximate value of the sensible heat flux is calculated, which is then substituted into the formulas (5), (6) to obtain the value of the Monin–Obukhov parameter. At the next iteration, the L value is substituted into the formula (4), and the calculations are being repeated until the calculated value of P flux differs from the value obtained at the previous step by 0.1 W/m^2.

The work [*Svyaschennikov, Ragulina, 2010*] analyzes the isothermality found in the upper layer of the Aldegonda Glacier during the ablation period; its thickness is 40–50 cm. The isothermal layer temperature corresponds to the melting point of ice. That makes it possible to determine the thickness of the ice layer melted during a day (in units of water equivalent) based on the heat flux spent on melting:

$$A_i = \frac{N_i \rho_i \Delta h_i}{\Delta t_i},$$

where A_i is the heat flux spent on melting, W/m^2; N_i is specific heat of ice melting, taken as $3.33 \cdot 10^5$ J/kg; ρ_i is ice density, taken equal to 916.7 kg/m^3; Δh_i is thickness of melted ice, mm w.e.; Δt_i is time interval, s.

Glaciological data. To verify modeling results, surface melting field observations data obtained on fourteen ablation stakes [*The study..., 2019*] evenly distributed over the glacier surface in almost all of its altitude range (Fig. 1), have been used. The surface melting values averaged over the glacier area have been calculated based on the ablation altitude profile obtained by linear approximation of melting values on individual stakes. The average values in fifty-meter altitude intervals are multiplied by the fraction of that altitudinal zone area in the total glacier area and summed up.

To calculate the error of ice ablation averaged over the glacier, we used the technique described in detail in the well-known work [*Klug et al., 2018*]. It includes two criteria: the standard deviation of the linear vertical dependence of ablation relative to field measurements, as well as the accuracy and representativeness of readings on the stakes. The error in ice density estimation is not taken into account.

RESULTS AND DISCUSSION

Quantitative evaluation of the heat balance and ice ablation components. As follows from Fig. 3, *a*, *b*, the average daily positive values of the surface heat balance components (shortwave budget (*2*) and turbulent heat transfer (*4*)) tend to decrease in their absolute values, which is associated with a decrease in the daylight hours duration and air temperature. The longwave budget of the surface does not have such a tendency (Fig. 3, *b*, *3*), since it is largely determined by the cloud cover value. Changes in the absolute value of the energy spent on ice melting (Fig. 3, *a*, *1*) generally repeat the fluctuations in the value of the shortwave budget of the surface, which clearly demonstrates its decisive role in melting on the glacier surface.

The spatial distribution of the radiation balance components (monthly mean values) during the period of maximum ablation is shown in Fig. 4. The shortwave balance, which is determined by the magnitude of incoming shortwave radiation (Fig. 4, *a*) and the albedo (Fig. 4, *b*), indicates that the greatest influx of solar radiation falls on to the northeastern part of the glacier. That is due to the azimuth and steepness of the glacier surface, as well as the greater, compared to other areas, shading of its southern part, and the minimum albedo at the glacier tongue and along the entire northern flank.

The longwave budget of the glacier surface during the ablation period is entirely determined by the atmospheric counter-radiation magnitude, since the longwave radiation from the surface directed upward

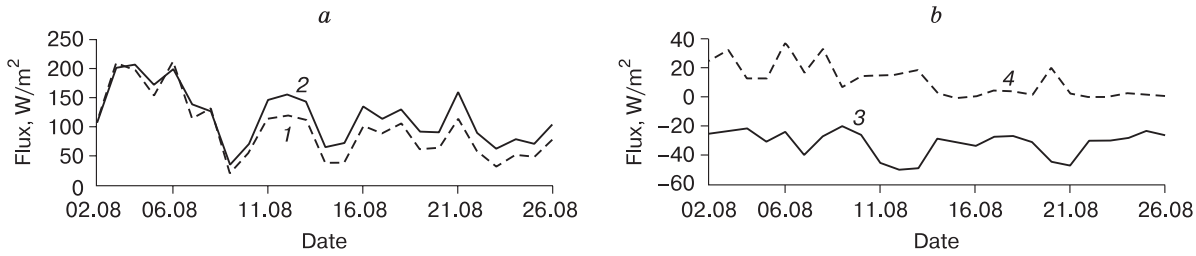

Fig. 3. Day-to-day variability of the heat balance components for the period from August 2 to 26, 2019.

a: heat consumption for ice melting (*1*), shortwave balance (*2*); *b*: longwave balance (*3*), turbulent heat exchange between the atmosphere and the underlying surface (*4*).

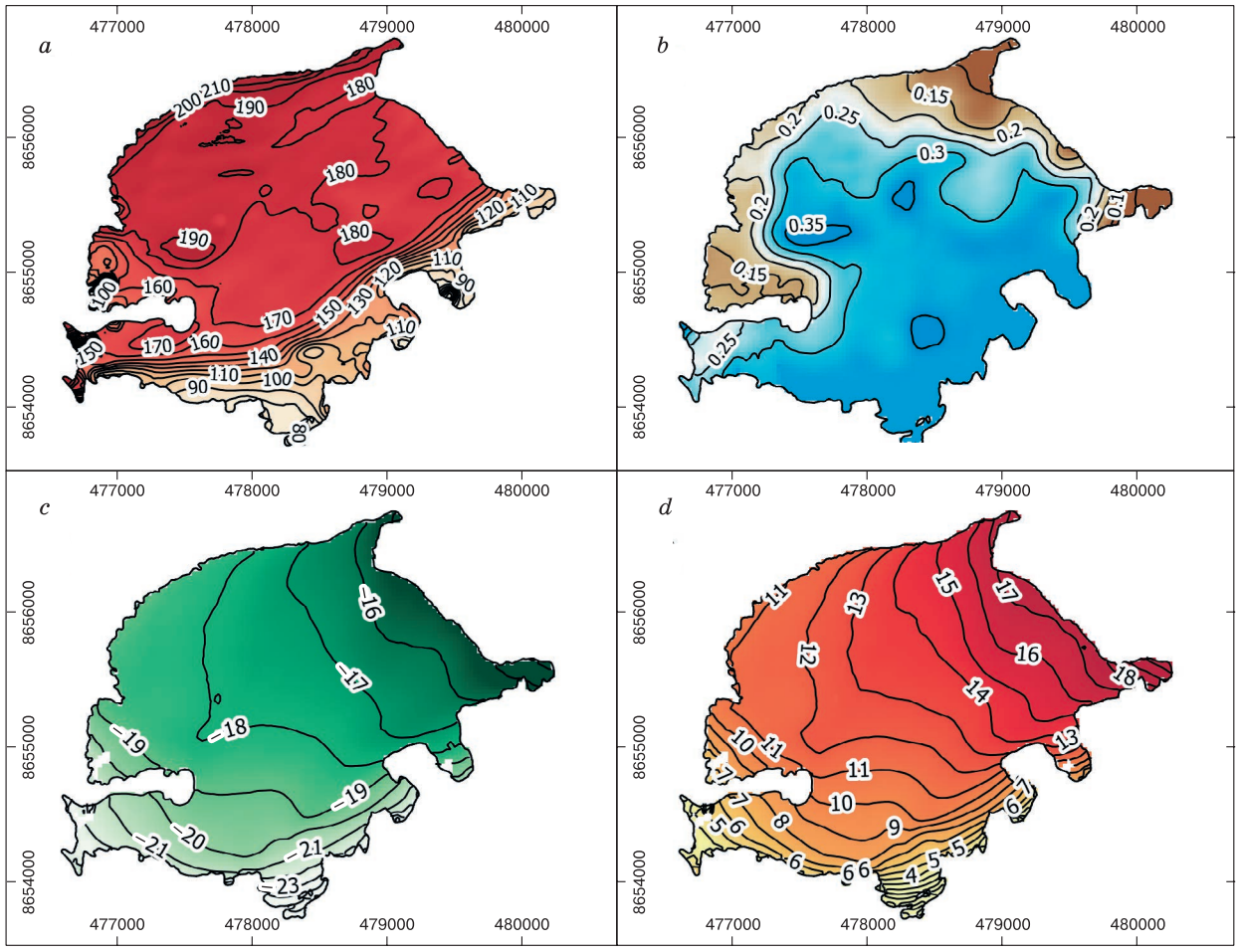

Fig. 4. Average monthly values of the heat balance components of the Aldegonda Glacier surface in August 2019.

a – incoming shortwave radiation (W/m^2); *b* – albedo of the underlying surface, in unit fractions; *c* – longwave balance of the surface (W/m^2); *d* – turbulent heat exchange between the underlying surface and the atmosphere (W/m^2). Coordinates are given in the UTM projection, Zone 33 on the WGS84 ellipsoid.

is assumed to be unchanged due to the constancy of measured melting-ice temperature. It follows from Fig. 4, *c* that the atmospheric counter-radiation decreases with the decreasing of the glacier surface altitude.

The maximum and minimum values of melting according to model calculations were correspondingly 1000–1200 mm w.e. per month, and 200–300 mm w.e. per month. According to our calculations, the main factor determining the spatial pattern of melting is the shortwave radiation balance of the glacier surface, since it is most variable in space. That is why the spatial distribution of surface melting (Fig. 5, *a*) largely repeats the spatial pattern of the albedo and incoming solar radiation distribution (Fig. 4, *a*, *b*).

There are several ways to assess the quantitative ratio of the heat balance components, depending on which value is taken as 100 %. The first method (used, for example, in [*Ohmura, 2001*]) is to find the share of each positive balance components of their sum. The ratio of components calculated in that way is shown in Table 1. In another approach [*Toropov et al., 2018*], the total radiation balance is considered as a separate component, and turbulent fluxes are considered as the other two. In comparison with the previous method, the share of turbulent fluxes greatly increases, since the radiation balance contains a negative component, – longwave radiation from the surface. The ratio of components calculated in this way is shown in Table 2.

In any case, turbulent heat transfer (Fig. 4, *d*, Table 1, 2) makes the smallest contribution, estimated at 3 % or 11 %, depending on the calculation method, which is almost an order of magnitude less than the radiation balance contribution. N.S. Arnold with

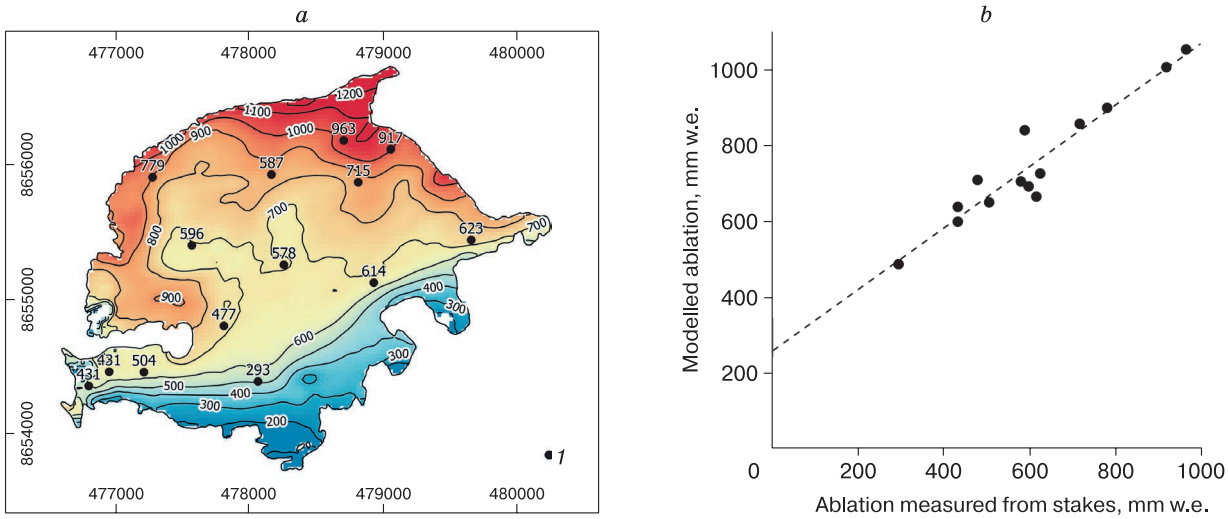

Fig. 5. Comparison of values of melting on the Aldegonda Glacier surface in August 2019 according to model and field data:

a – spatial distribution of melting (mm w.e.); *1* – ablation values measured from stakes (coordinates are given in the UTM projection zone 33 on the WGS84 ellipsoid); *b* – deviations of the simulation results from the actually measured values.

coauthors [*Arnold et al., 2006*] came to a similar conclusion for the Midtre Lovénbreen Glacier, located near Ny-Alesund (about one hundred kilometers to the north of Barentsburg) and comparable in size and altitude range to the Aldegonda Glacier.

Model verification. To assess the accuracy of the used model of the glacier surface heat balance, let us compare simulated and measured values of melting at the points of installation of the ablation stakes. In addition, we will calculate the average melting over the glacier surface, since this indicator is one of the main characteristics of the mass balance.

Figure 5, *b* is a scatter plot illustrating the relationship between the simulated and measured melting values for ablation stakes. The linear regression equation has the form of $y = 0.81x + 257.97$, the coefficients are significant ($p = 0.05$). The correlation coefficient is 0.95, the determination coefficient (R^2) is 0.90. On average, the ablation value at the glacier surface, obtained on the basis of the heat balance model, is 698 mm w.e./month, on stakes it is 615 ± 150 mm w.e./month. Thus, the model estimates of the average melting over the entire glacier surface fall within the confidence interval of the average value calculated based on field observations.

Possible sources of errors in model calculations. The absolute values of the differences between the calculated and measured values of melting, according to the authors, are not informative enough for analyzing the sources of errors, since both values are multiplied by a conversion factor equal to ice to water density ratio for conversion to water equivalent units. Here the ice was taken as the maximum possible (916.7 kg/m^3), although, in general the ice on the glacier surface is less dense due to the inclusion of air bubbles. Using a different ice density value will proportionally reduce those differences. Therefore, the authors tried to estimate the errors of the model in the heat flux values, but not in the melted layer thickness, thereby excluding the ice density as an additional factor introducing the error. Based on measured ablation values, the heat amount necessary to ensure that melting bas been calculated (Fig. 6).

It follows from Fig. 6, *a* that, despite the high value of correlation coefficient, the model systematically overestimates the heat losses for ice melting relative to those measured using ablation stakes, and that difference changes with glacier surface altitude (Fig. 6, *b*). In our case, the difference increases from about 10 to 30 W/m^2. Several factors can explain

Table 1. **The ratio of the heat balance components of the Aldegonda Glacier, calculated in accordance with [*Ohmura et al., 2001*]**

Absorbed shortwave radiation		Downwelling longwave radiation		The sum of turbulent fluxes	
W/m^2	%	W/m^2	%	W/m^2	%
121	29	278	68	11	3

Table 2. **The ratio of the heat balance components of the Aldegonda Glacier, calculated in accordance with [*Toropov et al., 2018*]**

Radiation balance		Sensible heat flux		Latent heat flux	
W/m^2	%	W/m^2	%	W/m^2	%
89	89	10	10	1	1

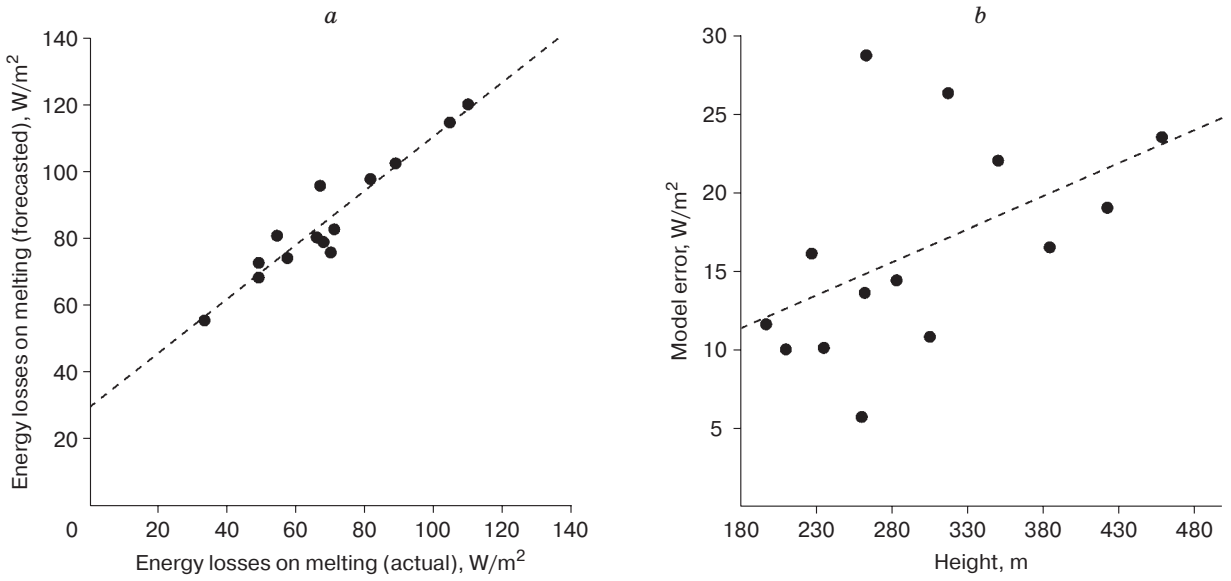

Fig. 6. Model error in the units of heat flux:

a – deviations of simulation results from measured values; *b* – their altitude dependence.

that. Since the largest positive part of the heat balance components is the incoming shortwave solar radiation, the model becomes most sensitive to errors in estimating this component. In particular, the underestimated albedo can introduce a significant part of the error. Because of the peculiarities of the glacier's exposure and the configuration of surrounding terrain, the shaded area at this season increases with altitude. It is known [*Liang, 2001*] that the surface reflectivity values obtained from satellite data can be underestimated in areas with low illuminance. Nevertheless, it is not entirely correct to associate model errors only with inaccuracy in determining the albedo. With the value of incoming shortwave radiation average for the observation period equal to about 250 W/m^2, the systematic error in calculating the albedo should be, averaged over the glacier surface, at least 10 %, which is unrealistically high.

The next possible source of errors is the structure of the surface ice layer which is not taken into account in a model. First, the heat flux from the isothermal layer into the underlying glacier layers is not taken into account due to its thermal conductivity. However, the magnitude of such a flux during the period of maximum ablation is no more than –5 W/m^2 for a mountain glacier located in similar climatic conditions [*Hock, Holmgren, 1996*], but can amount only to some part of model error. Second, the model does not take into account the penetration of shortwave radiation into the ice (into the radiation active layer). A significant part of solar energy, primarily in the ultraviolet and near infrared parts of the spectrum, is absorbed directly below the surface of the glacier, since the penetration of energy into the stratum rapidly decreases exponentially with depth in accordance with the Bouguer–Lambert law. However, some part of the shortwave radiation penetrates below the isothermal layer, which introduces a systematic positive error into the model, revealed based on field data.

Thus, the authors associate the further development of the heat balance model of glacier melting with a more detailed description (parameterization) of the processes associated with heat transfer deep into the glacier, and with a more realistic description of surface ice layer density and structure.

CONCLUSION

The modeled estimates of the spatial distribution of ablation values were compared with the results of field measurements using ablation stakes for the same period. The correlation coefficient was 0.95, and the determination coefficient (R^2) was 0.90. The magnitude of the glacier surface ablation, obtained based on the heat balance model, averaged 698 mm w.e./month. A similar value obtained from the stakes is 615 ± 150 mm w.e./month. Thus, the model estimates do not go beyond the confidence interval of estimates obtained based on field observations.

According to the authors' calculations, the main factor determining melting is the radiation balance of the glacier surface, and the turbulent heat transfer makes an order of magnitude smaller contribution to melting (3 % to 11 %, depending on the method of estimating the component ratio). A similar result has been obtained in a number of other works [*Arnold et al., 2006; Van As, 2011; Jakobs et al., 2019*]. The pat-

tern of melting spatial distribution largely repeats that of the albedo and incoming solar radiation distribution, since it is those values that have the greatest variability on the glacier surface.

Acknowledgments. *The authors are grateful to the participants and the leadership of the "Spitsbergen-2019" RAE-S expedition for help in organizing and performing seasonal field work.*

The work was performed within the framework of theme 5.1.4 of the R&D plan of the Roshydromet.

References

Arnold, N.S., Rees, W.G., Hodson, A.J., Kohler, J., 2006. Topographic controls on the surface energy balance of a high Arctic valley glacier. J. Geophys. Res.: Earth Surface, vol. 111, No. F2.

Beljaars, A.C.M., Holtslag, A.A.M., 1991. Flux parameterization over land surfaces for atmospheric models. J. Appl. Meteor. 30, 327–341.

Böhner, J., Antonić O., 2009. Land surface parameters specific to topo-climatology. Developm. Soil Sciences 33, 195–226.

Chernov, R.A., Kudikov, A.V., Vshivtseva, T.V., Osokin, N.I., 2019. Estimation of the surface ablation and mass balance of Eustre Grønfjordbreen (Spitsbergen). Led i Sneg [Ice and Snow], 59 (1), 59–66 (in Russian).

Førland, E.J., Isaksen, K., Lutz, J., et al., 2020. Measured and modeled historical precipitation trends for Svalbard. J. Hydrometeor. 21, 1279–1296.

Gjelten, H.M., Nordli, Ø., Isaksen, K., et al., 2016. Air temperature variations and gradients along the coast and fjords of western Spitsbergen. Polar Research 35, p. 29878.

Hock, R., 2003. Temperature index melt modelling in mountain areas. J. Hydrol. 282, 104–115.

Hock, R., 2005. Glacier melt: a review of processes and their modelling. Progress in Phys. Geography 29 (3), 362–391.

Hock, R., Holmgren, B., 1996. Some aspects of energy balance and ablation of Storglaciaren, northern Sweden. Geografiska Ann.: Ser A, Physical Geography 78 (2–3), 121–131.

Isaksen, K., Nordli, Ø., Førland, E.J., et al., 2016. Recent warming on Spitsbergen – Influence of atmospheric circulation and sea ice cover. J. Geophys. Res. Atmos. 121 (11), 913–931.

Ivanov, B.V., Svyashchennikov, P.N., 2015. Albedo of the snow-glacier surface of Svalbard. Izvestiya, Atmospheric and Oceanic Phys. 51 (9), 943–948.

Jakobs, C.L., Reijmer, C.H., Kuipers Munneke, P., et al., 2019. Quantifying the snowmelt-albedo feedback at Neumayer Station, East Antarctica. The Cryosphere 13 (5), 1473–1485.

Karner, F., Obleitner, F., Krismer, T., et al., 2013. A decade of energy and mass balance investigations on the glacier Kongsvegen, Svalbard. J. Geophys. Res.: Atmospheres 118 (10), 3986–4000.

Klok, E., Oerlemans, J., 2002. Model study of the spatial distribution of the energy and mass balance of Morteratschgletscher, Switzerland. J. Glaciol. 48 (163), 505–518.

Klug, C., Bollmann, E., Galos, S.P., et al., 2018. Geodetic reanalysis of annual glaciological mass balances (2001–2011) of Hintereisferner, Austria. The Cryosphere, 12, 833–849.

König-Langlo, G., Augsteine, E., 1994. Parameterization of the downward long-wave radiation at the Earth's surface in polar regions. Meteorologische zeitschrift 3 (6), 343–347.

Krenke, A.N., Khodakov, V.G., 1966. On the connection between surface melting of glaciers and air temperature. Materialy Glyatsiologicheskikh Issledovaniy [Data of Glaciological Studies], No. 12, 153–164 (in Russian).

Liang, S., 2001. Narrowband to broadband conversions of land surface albedo I: Algorithms. Remote Sens. Environ. 76, 213–238.

Munro, D.S., 1990. Comparisons of melt energy computations and ablatometer measurements on melting ice and snow. Arct. Alp. Res. 22 (2), 153–162.

Naegeli, K., Damm, A., Huss, M., et al., 2017. Cross-Comparison of albedo products for glacier surfaces derived from airborne and satellite (Sentinel-2 and Landsat 8) optical data. Remote Sens. 9 (2), article 110.

Naegeli, K., Huss, M., Hoelzle, M., 2019. Change detection of bare-ice albedo in the Swiss Alps. The Cryosphere 13, 397–412.

Nordli, Ø., Przybylak, R., Ogilvie, A.E.G., Isaksen, K., 2014. Long-term temperature trends and variability on Spitsbergen: the extended Svalbard Airport temperature series, 1898–2012. Polar Res. 33 (1), p. 21349.

Ohmura, A., 2001. Physical basis for the temperature-based melt-index method. J. Appl. Meteorol. 40, 753–761.

Rets, E.P., Frolova, N.L., Popovnin, V.V., 2011. Modelling of surface ablation of a mountain glacier. Led i Sneg [Ice and Snow], 51 (4), 24–31 (in Russian).

Schuler, T.V., Kohler, J., Elagina, N., et al., 2020. Reconciling Svalbard glacier mass balance. Frontiers in Earth Sci., vol. 8, article 156.

Svyaschennikov, P.N., Ragulina, G.A., 2010. Estimation of surface ablation of Aldegonda glacier, Svalbard archipelago. In: Nature of shelves and archipelagos of the European Arctic. Comprehensive studies of Svalbard nature. GEOS, Moscow, pp. 469–474 (in Russian).

The study of present-day state and the analysis of past changes of characteristics of Svalbard archipelago environment: Scientific report (final report), 2019. In: Scientific Report. Arctic and Antarctic Research Institute Repository ID No. P-6596. Saint Petersburg, 247 pp. (in Russian).

Toropov, P.A., Shestakova, A.A., Smirnov, A.M., Popovnin, V.V., 2018. Evaluation of the components of the heat balance of the Djankuat glacier (Central Caucasus) during the period of ablation in 2007–2015. Earth's Cryosphere XXII (4), 37–48.

Van As, D., 2011. Warming, glacier melt and surface energy budget from weather station observations in the Melville Bay region of northwest Greenland. J. Glaciol. 57 (202), 208–220.

Van Pelt, W.J.J., Oerlemans, J., Reijmer, C.H., et al., 2012. Simulating melt, runoff and refreezing on Nordenskiöldbreen, Svalbard, using a coupled snow and energy balance model. The Cryosphere 6, 641–659.

Voloshina, A.P., 1966. Heat balance of a surface of high-mountain glaciers during summer period: case study of Elbrus. Nauka, Moscow, 150 pp. (in Russian).

Voloshina, A.P., 2001. Meteorology of the mountain glaciers. Materialy Glyatsiologicheskikh Issledovaniy [Data of Glaciological Studies], No. 92, 3–138 (in Russian).

Wheler, B.A., Flowers, G.E., 2011. Glacier subsurface heat-flux characterizations for energy-balance modelling in the Donjek Range, southwest Yukon, Canada. J. Glaciol. 57 (201), 121–133.

Received September 22, 2020
Revised version received January 17, 2021
Accepted January 19, 2021